

Pyrolysis of Waste Fryer Grease in a Fixed-Bed Reactor

Adenike Adebajo, Mangesh G. Kulkarni, Ajay K. Dalai,* and Narendra N. Bakhshi

Catalysis and Chemical Reaction Engineering Laboratories, Department of Chemical Engineering,
University of Saskatchewan, Saskatoon, Canada

Received May 25, 2006. Revised Manuscript Received November 17, 2006

Waste fryer grease (WFG) is an environmentally preferable option for hydrogen production. In the present work, the pyrolysis of waste fryer grease in the absence of catalyst was studied in a fixed-bed reactor. The effects of various operating parameters such as reaction temperature (650–850 °C), carrier gas (N₂) flow rate (30–70 mL/min), and reactor inert packing particle size (0.5–2.5 mm) on hydrogen and syngas (i.e., mixture of H₂ + CO) production were studied. Quadratic response surface models used in analyzing the product gas and char data showed that temperature was the most important parameter over the wide range of conditions studied. The effect of particle size on the product gas and char yield was not significant. Residence time influenced both hydrogen and syngas composition, but its effect was smaller than that of temperature. Numerical optimization of the responses gave a composition of 17.8 mol % for hydrogen, 26.6 mol % for syngas, and a char yield of 13.7 g/100 g of waste fryer grease. Steam was introduced in the reaction system to increase the hydrogen production. The addition of steam (a steam to carbon ratio of 1.5) caused a drastic increase in the hydrogen production to a maximum of 56.2 mol % and in syngas to a maximum of 82.4 mol %.

1. Introduction

Petroleum based fuels are major fuels used worldwide. Two major threats to these fuels in near future are depletion of feedstocks and the atmospheric pollution created by consumption of fossil fuels. Petroleum diesel combustion is a major source of air contaminants such as greenhouse gas (GHG), NO_x, SO_x, CO, particulate matter, and volatile organic compounds.¹ In view of these two disadvantages, worldwide research is focused on developing new technologies for the generation of alternative energy.

Biofuels obtained from biomass may be considered as one of the most promising alternatives to fossil fuels. These fuels include liquid fuels mainly ethanol, biodiesel and Fischer–Tropsch diesel, and gaseous fuels such as hydrogen and methane. Out of all the liquid and gaseous biofuels, hydrogen is most attractive source of alternative energy for the 21st century because of its environmentally benign nature. Currently, most hydrogen is being produced from natural gas,² with CO₂ as a major byproduct, which is responsible for the greenhouse effect. For example, life-cycle analysis of the production of hydrogen in a steam reforming plant based on natural gas with a capacity of 1.5×10^6 Nm³/d shows that the amount of fossil CO₂ equivalent released into the atmosphere to produce 100 kg of hydrogen gas is 1374.4 kg.³ Biomass is an environmentally friendly and renewable resource for hydrogen production. Biomass generally contains carbon, hydrogen, and oxygen along with some moisture. Under controlled conditions characterized by low oxygen supply and high temperatures, most biomass materials can be converted via thermochemical processes into a gaseous fuel which consists of hydrogen, carbon dioxide (CO₂), carbon monoxide (CO), methane, etc. The CO₂ released

during the thermochemical conversion of biomass is offset by the uptake of CO₂ during biomass growth.³

Waste fryer grease (used cooking oil) has a great potential for the production of biofuels. Cooking oil undergoes many physical and chemical changes and produces many undesirable chemicals after a number of repetitive fryings and cannot be used for edible purposes.^{4–5} Previously, these waste oils were used as animal feed. Since 2002, its use as animal feed has been banned in Europe and other countries,⁶ and its disposal is also problematic. Therefore, it becomes mandatory to find some alternative uses for the waste cooking oil. The production of biofuels such as biodiesel is one of the most attractive and efficient utilizations of waste fryer grease.⁷ However, efforts to make biodiesel from waste fryer grease are plagued due to the presence of undesirable compounds in it, especially free fatty acids (FFA) and water. Also, the undesirable products such as dimers and trimers formed during frying have an adverse effect on some of the biodiesel properties such as Conradson carbon residue (CCR).⁸ In addition to these serious disadvantages, biodiesel obtained from waste fryer grease also produces more NO_x when tested in commercial diesel engines.⁹ Hence, utilization of waste fryer grease for biodiesel production is very limited and it depends on the extent of damage done to the cooking oil during frying. Although the production of biodiesel from waste fryer grease is well reported in the literature, its utilization for gaseous fuel production especially hydrogen/syngas is not well reported.

Cracking of waste vegetable oil to produce liquid and gaseous fuels has been studied by Czernik et al.³ Steam reforming of

* Corresponding author. E-mail: ajay.dalai@usask.ca. Tel.: (306) 966-477. Fax: (306) 966-4777.

(1) Klass, L. D. Academic Press: New York, 1998. p. 1.

(2) Nath, K.; Das, D. *Curr. Sci.* **2003**, 85 (3), 265–270.

(3) Czernik, S.; French, R. J.; Magrini-Bair, K. A.; Chornet, E. *Energy Fuels* **2004**, 18, 1738–1743.

(4) Nawar, W. W. *J. Chem. Educ.* **1984**, 61, 299–302.

(5) Guesta, F.; Sanchez-Muniz, J. *J. Am. Oil Chem. Soc.* **1993**, 7, 1069–1073.

(6) Cvengros, J.; Cvengrosova, Z. *Biomass Bioenergy* **2004**, 27, 173–181.

(7) Nye, M. J.; Williamson, T. W.; Deshpande, S. *J. Am. Oil Chem. Soc.* **1983**, 60, 1598–1601.

(8) Dorado, M. P.; Ballesteros, E.; Arnal, J. M.; Gomez, J.; Lopez, F. J. *Fuel* **2003**, 82, 1311–1315.

trap grease (recovered from traps installed in the sewage lines of restaurants, food processing plants, and wastewater treatment plants) was carried out to produce hydrogen for over 150 h in a fluidized bed reactor at 850 °C with a steam to carbon (S/C) ratio of 5 and a methane equivalent space velocity of 1000 h⁻¹ using a commercial nickel based (C11-NK) naphtha reforming catalyst. Approximately 25 g of hydrogen per 100 g of feed was produced. However, it was observed that the process performance was seriously affected over time because of catalyst attrition and deactivation.³ The physical loss and poisoning of the catalyst were serious problems due to the presence of a number of undesirable compounds in the waste vegetable oil.

The cracking of waste palm oil to produce organic liquid product enriched with gasoline fraction was carried out using MCM-41/zeolite Beta composite material.¹⁰ The activity test was carried out at a reaction temperature of 450 °C and a feed rate of waste used palm oil of 2.5 g/h at atmospheric pressure in a fixed-bed microreactor containing 1 g of catalyst. The gaseous products mainly consisted of propane, propylene, butane, and butylenes while the organic liquid product consisted of gasoline, kerosene, and diesel fractions. The yield of the gasoline fraction was up to 35.2 wt % of the total products.

Most of the studies,^{9–12} on the cracking of waste fryer grease (WFG) have used commercial cracking catalyst to produce either gaseous or liquid products. However, as discussed earlier, WFG is usually contaminated with a number of undesirable compounds. The nature and effects of most of these compounds are not fully known. Also, the composition of WFG changes with changes in the source of the oil. Hence, these unknown compounds can seriously affect the performance of the process and catalyst over long periods, which can create problems during the commercialization of this process.

The pyrolysis of WFG in the absence of catalyst over an inert material has not been studied so far. In the present work, the pyrolysis of WFG in a fixed-bed reactor over an inert material is studied. The effects of various reaction parameters such as the reaction temperature (650–850 °C), carrier gas flow rate (30–70 mL/min), and particle size (0.5–2.5 mm) on hydrogen, syngas, and char production were investigated in detail. The central composite design of experiments was used to construct second-order response surfaces for the hydrogen, syngas, and char production as optimization parameters. The main objective of the work is to maximize both hydrogen and syngas production and to minimize the char yield. In order to enhance the hydrogen and syngas yields, steam gasification of the WFG was also carried out. The overall objective of the work is to utilize WFG efficiently for the production of hydrogen or syngas.

2. Experimental

The waste fryer grease (WFG) was supplied by Saskatoon Processing Co., Saskatoon. It was treated with citric acid to remove the solid particles. The carbon (C), hydrogen (H), and nitrogen (N) analysis of the WFG was performed on a CHN analyzer (Perkin-Elmer 2400).

2.1. Pyrolysis and Steam Gasification of Waste Fryer Grease. Pyrolysis of WFG was conducted at atmospheric pressure in a continuous fixed-bed microreactor (310 mm long, 10 mm i.d.) made

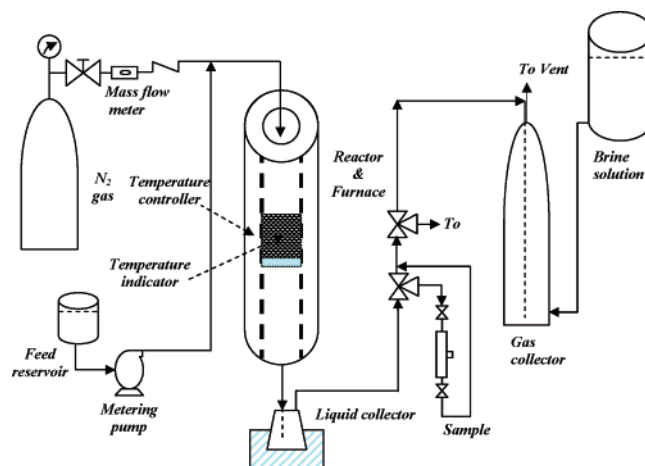


Figure 1. Schematic diagram of experimental setup for pyrolysis of waste fryer grease.

up of Inconel. Quartz particles with a packing height of 70 mm were held on a plug of quartz wool placed on a supporting mesh inside the microreactor. The experimental set up is shown in Figure 1. The reactor was heated by a furnace equipped with an autotuning proportional–integral–derivative (PID) temperature controller (Shimaden Co. Ltd., Tokyo, Japan) using a K-type thermocouple placed on the furnace side of the annulus between the furnace and the reactor. Another thermocouple (in a thermowell) was used to monitor the temperature at the center of the reactor. The WFG was fed to the reactor using a programmable syringe pump (Genie model YA-12) at a flow rate of 5 g/h. The desired flow rate of the carrier gas (N₂) was maintained by using a mass flow meter (Top-trak model 822). Each experiment was run for 0.5 h in which there was very little variation of product gas compositions. The liquid products were collected with the help of a condenser attached to the bottom of the reactor outlet. The gaseous products were collected in a gas collector by the downward displacement of a brine solution. The saturated brine solution was used to prevent CO₂ dissolution in pure water. After each run, the reactor was cooled and weighed to determine the amount of retained products (char). The condensate was also weighed for mass balance purposes. Experiments were also repeated under same reaction conditions in order to see the reproducibility of the results.

In order to improve on hydrogen production, steam gasification of the WFG was conducted at the optimum temperature obtained in the pyrolysis experiment. No carrier gas was used during this process. Since WFG is not miscible with water, another syringe pump was used to pump the water required to produce the required steam for the gasification.

2.2. Gas Product Analysis. The product gas was analyzed for its composition using two gas chromatographs (GCs, HP5890 and HP5880). The HP5890 was equipped with a thermal conductivity detector (TCD) and a Carbowise S II column and was used to analyze H₂, CO, CO₂, and CH₄. The conditions used for the HP5890 were as follows: initial temperature of 40 °C, initial temperature hold time of 1 min, heating rate of 12 °C/min, final temperature of 200 °C, final temperature hold time of 1 min, and detector temperature of 250 °C. The HP5880 GC equipped with a flame ionization detector and a SP2100 column was used to analyze hydrocarbons. The conditions used for the HP5880 were as follows: initial temperature of 40 °C, initial temperature hold of 3 min, column heating rate of 10 °C/min, final temperature of 200 °C, final hold time of 2 min, and detector temperature of 250 °C. The gas analysis was done on a carrier gas (N₂) free basis.

2.3. Statistical Design of Experiment. Statistical design of an experiment is usually done to identify the experimental factors which will minimize the effects of uncontrolled factors on the responses. According to previous studies on pyrolysis in fixed-bed reactors,^{13–16} temperature, residence time, and packing particle size are influential factors on pyrolysis reactions and products. To study

(9) Mittelbach, M.; Enzelsberger, H. *J Am. Oil Chem. Soc.* **1999**, *76*, 545–550.

(10) Ooi, Y.; Zakaria, R.; Mohamed, A. R.; Bhatia, S. *Appl. Catal., A* **2004**, *274*, 15–23.

(11) Czernik, S.; French, R.; Feik, C.; Chornet, E. *Ind. Eng. Chem. Res.* **2002**, *41*, 4209–4215.

(12) Ooi, Y.; Zakaria, R.; Mohamed, A. R.; Bhatia, S. *Energy Fuels* **2004**, *18*, 1555–1561.

Table 1. Actual and Coded Levels of the Design Parameters

<i>T</i> (°C)	600	650	750	850	900
carrier gas flow rate (mL/min)	20	30	50	70	80
packing particle size (mm) ^a	0.0	0.5	1.5	2.5	3.0
codes	−*	−1	0	+1	+

^a A range of particle sizes was used, and the given value is an approximate median of the range; an empty reactor was used for the zero particle size.

the effects of these factors and to obtain a predictive model on hydrogen and syngas composition in the product gas, heating value of the product gas, and char yield, the response surface methodology (RSM) was used via the central composite circumscribed (CCC) design. The software package used was Stat-Ease Design Expert-Software, version 6.

The RSM is a collection of mathematical and statistical techniques with the objective of optimizing the response. The first step in RSM is to find an approximation of the true relationship between the response and the set of independent variables. The response is usually modeled by a low-level polynomial (first-order or second-order) that usually works relatively well under a relatively small region. Contour plots play a very important role in response surface methods. By use of this technique, one can characterize the shape of the surface and locate the optimum point with reasonable precision.

The central composite design consists of an embedded factorial and fractional factorial design, characterized by central (0), axial (−1, +1), and star points (*). As shown in Table 1, coded points represent the actual data in terms of −1 and +1, i.e., minimum and maximum which can be calculated as

$$CPV = -1 + \frac{(APV - APV_{\min})}{0.5(APV_{\max} - APV_{\min})} \quad (1)$$

where APV is the actual product value and CPV is the coded product value.

The star points represent the extreme values of each design factor which are used to analyze the curvature in the response. The CCC designs are the original form of the central composite design. Table 1 also shows the actual levels of the design factors used for the pyrolysis of WFG. The number of trials (*N*) was based on the number of the design factors (*k* = 3) as follows:

$$N = 2^k + 2k + 3 = 17 \text{ trials} \quad (2)$$

where 3 is the number of replicates at the center level.

The analysis of variance (ANOVA) technique was chosen to estimate the fitness of the regression models. This is a test based on the variance ratios to determine whether or not significant differences exist among the means of several groups of observation.¹⁷ The *F* statistic was used to evaluate the overall performance of the models. A poor regression will have a low value for *F*. The *F* value may be viewed as a measure of the signal-to-noise ratio in the model.¹⁸ The lack-of-fit test was used to determine whether the regression models were adequate to describe the observed data. A significant lack-of-fit (*p* value < 0.1) is not desired for the model. It shows that there are some contributions from the response–input relationship that are not explained by the model.¹⁹ The *R*-squared

statistics indicates the percentage of the variability of the optimization parameter that is explained by the model.²⁰ In addition, the adequacy of the model is also investigated by the examination of residuals.²¹ The residuals, which are the difference between the respective, observed responses and the predicted responses, are examined using the normal probability plots of the residuals and the plots of the residuals versus the predicted response. If the model is adequate, the points on the normal probability plots of the residuals should form a straight line. On the other hand, the plots of the residuals versus the predicted response should contain no obvious patterns.¹⁹

3. Results and Discussion

The overall elemental analysis (on a mass basis) of the waste fryer grease (WFG) gave 77.8% carbon, 11.2% hydrogen, and 11.0% oxygen (obtained by difference). No nitrogen or sulfur was detected in the WFG. The elemental analysis of biomass plays crucial role in gasification since it may indicate how much maximum hydrogen/syngas can be generated from the particular feedstock. The elemental composition of the biomass depends on many factors such as its type, soil conditions, climate, and storage etc.

Liquid, gas, and char are three products obtained during pyrolysis of the WFG. The liquid product contains aromatics, alcohols, ketones, etc., whereas the gaseous product contains mostly CO, CO₂, H₂, C_{1–4}, and hydrocarbons. The weight percentage of each product obtained under the different reaction conditions (17 trials) is as shown in Table 2. The material balance under all the experimental conditions was between 90 and 93% with good reproducibility. The low material balance is because of the complexity in the collection and analysis of products (gaseous and liquid). There were three experiments performed at 750 °C with a carrier gas flow rate of 50 mL/min and a quartz particle size of 1.5 mm with a feed flow rate of 5.4–5.8 g/h. In these cases, the gas, liquid, and char product yields were 76.1 ± 2.5, 14.7 ± 2.2, and 5.6 ± 3.6, indicating the reproducibility of the results in the production of gas and liquid. However, in terms of char production, the error seems high which indicates that the experiments are not very reproducible in terms of char. The fact that the waste fryer grease can be unstable over time may account for the variability in the gas product, gas composition, and char yield. The effects of the reaction parameters on hydrogen/syngas and char production are discussed in detail as follows:

3.1. Analysis of Variance. The analysis of variance (ANOVA) (Table 3) is used to summarize the results obtained under all the experimental conditions. All the models were modified by reducing the terms that are not significant by manual elimination. No transformation was required to obtain an insignificant lack of fit for hydrogen and syngas concentrations and char yield models. However, the inverse transformation was necessary to obtain an insignificant lack-of-fit for the product gas heating value model.

The ANOVA table (see Table 3) describes the response surface reduced quadratic model used for different response parameters as hydrogen and syngas concentration in the product gas, char yield, and heating value of the product gas. It is evident from this table that the effects of temperature (*A*) and carrier gas flow rate (*B*) are the two factors affecting hydrogen/syngas concentration. However, statistical analysis also showed that the second-order (*A*²) effect of temperature is significant as can

(13) Idem, R. O.; Katikaneni, S. P. R.; Bakhshi, N. N. *Energy Fuels* **1996**, *10*, 1150–1162.

(14) Adebajo, A. O.; Dalai, A. K.; Bakhshi, N. N. *Energy Fuels* **2005**, *19*, 1735–1741.

(15) Valliyappan, T. M.Sc. Thesis, University of Saskatchewan, Canada, 2004.

(16) Demirbas, A. *J. Anal. Appl. Pyrolysis* **2004**, *72*, 215–219.

(17) Wang, L. Y.; Park, J. S.; Jung, H.; Lee, H. T.; Lee, D. K. *Fuel* **1999**, *78*, 809–813.

(18) Zhuo, Y.; Lemaigen, L.; Chatzakos, I. N.; Reed, G. P.; Dugwell, D. R.; Kandiyoti, R. *Energy Fuels* **2000**, *14*, 1049–1058.

(19) Noordin, M. Y.; Venkatesh, V. C.; Sharif, S.; Elting, S.; Abdullah, A. *J. Mater. Process Technol.* **2004**, *145*, 46–58.

(20) Rigas, F.; Panteleos, P.; Laoudis, C. *Global Nest Intl. J.* **2004**, *2*, 245–253.

(21) Montgomery, D. C. *Design and Analysis of Experiments*, 4th ed.; Wiley: New York, 1997.

Table 2. Material Balance during the Pyrolysis of Waste Fryer Grease in a Fixed-Bed Reactor^a

temp (°C)	carrier gas (N ₂) (mL/min)	quartz particle size (mm)	WFG feed (g)	gas product		liquid product		char		mass balance	
				(g)	(wt %)	(g)	(wt %)	(g)	(wt %)	(g)	(wt %)
900	50	1.5	2.4	1.4	62.1	0.3	14.4	0.5	24.0	2.2	91
750	50	1.5	2.2	1.5	76.1	0.3	14.7	0.2	9.2	2.0	91
850	70	0.5	2.5	1.7	73.3	0.4	15.7	0.2	11.0	2.3	90
650	70	0.5	2.4	1.3	58.7	0.6	27.1	0.3	14.2	2.2	91
650	30	0.5	2.5	1.7	70.5	0.4	18.5	0.2	11.0	2.3	90
850	30	2.5	2.6	1.7	71.6	0.4	15.0	0.3	13.4	2.4	90
650	30	2.5	2.5	1.4	63.6	0.6	25.3	0.3	11.1	2.3	90
600	50	1.5	2.5	1.0	41.8	1.2	50.3	0.2	7.9	2.3	90
750	20	1.5	2.4	1.7	77.8	0.3	14.5	0.2	7.7	2.2	91
750	50	1.5	2.4	1.7	79.8	0.3	14.6	0.1	5.6	2.1	90
750	50	0.0 ^b	2.5	1.6	71.4	0.4	19.6	0.2	9.0	2.3	90
650	70	2.5	2.5	1.7	72.2	0.5	20.4	0.2	7.4	2.3	90
750	50	3.0	2.5	1.8	78.3	0.3	15.1	0.1	6.7	2.3	90
850	30	0.5	2.5	1.5	65.3	0.4	16.5	0.4	18.2	2.3	90
750	50	1.5	2.3	1.7	78.7	0.3	12.5	0.2	8.8	2.2	93
750	80	1.5	2.5	1.9	80.2	0.2	7.8	0.3	12.0	2.3	90
850	70	2.5	2.5	1.7	69.4	0.4	16.2	0.3	14.4	2.3	90

^a Basis run time 30 min ^b No quartz particles in the reactor.

Table 3. Analysis of Variance Table for the Reduced Quadratic Model

source	sum of squares	DF	mean square	F value	prob > F	
Hydrogen Concentration ^a						
model	785.78	3	261.93	148.99	<0.0001	significant
A	698.93	1	698.93	397.57	<0.0001	
B	26.04	1	26.04	14.81	0.0020	
A ²	60.81	1	60.81	34.59	<0.0001	
residual	22.85	13	1.76			
lack of fit	22.38	11	2.03	8.65	0.1081	not significant
pure error	0.47	2	0.24			
cor total	808.63	16				
Syngas Concentration ^b						
model	747.02	3	249.01	97.96	<0.0001	significant
A	675.06	1	675.06	265.56	<0.0001	
B	29.88	1	29.88	11.75	0.0045	
A ²	42.09	1	42.09	16.56	0.0013	
residual	33.05	13	2.54			
lack of fit	31.13	11	2.83	2.95	0.2805	not significant
pure error	1.92	2	0.96			
cor total	780.07	16				
Char Yield ^c						
model	178.49	2	89.24	13.17	0.0006	significant
A	88.71	1	88.71	13.09	0.0028	
A ²	89.78	1	89.78	13.24	0.0027	
residual	94.90	14	6.78			
lack of fit	88.69	12	7.39	2.38	0.3336	not significant
pure error	6.21	2	3.10			
cor total	273.38	16				
Heating Value of Product Gas (Inverse Transformation) ^d						
model	2.58 × 10 ⁻⁴	4	6.46 × 10 ⁻⁵	98.69	<0.0001	significant
A	2.23 × 10 ⁻⁴	1	2.23 × 10 ⁻⁴	340.67	<0.0001	
B	9.18 × 10 ⁻⁶	1	9.18 × 10 ⁻⁶	14.02	0.0028	
A ²	2.48 × 10 ⁻⁵	1	2.48 × 10 ⁻⁵	37.91	<0.0001	
AB	1.42 × 10 ⁻⁶	1	1.42 × 10 ⁻⁶	2.16	0.1672	
residual	7.86 × 10 ⁻⁶	12	6.55 × 10 ⁻⁷			
lack of fit	7.69 × 10 ⁻⁶	10	7.69 × 10 ⁻⁷	9.19	0.1021	not significant
pure error	1.67 × 10 ⁻⁷	2	8.37 × 10 ⁻⁸			
cor total	2.66 × 10 ⁻⁴	16				

^a Std dev = 1.3, mean = 8.2, C.V. = 16.2, R² = 0.97, adj R² = 0.97, pred R² = 0.94, adeq precision = 36.4. ^b Std dev = 1.6, mean = 17.2, C.V. = 9.3, R² = 0.96, adj R² = 0.95, pred R² = 0.91, adeq precision = 29.3. ^c Std dev = 2.6, mean = 10.2, C.V. = 25.6, R² = 0.065, adj R² = 0.60, pred R² = 0.34, adeq precision = 10.2. ^d Std dev = 8.1 × 10⁻⁴, mean = 0.01, C.V. = 5.8, R² = 0.97, adj R² = 0.96, pred R² = 0.92, adeq precision = 29.8.

be inferred from the probability values which are much less than 0.1. The results imply that the hydrogen concentration, syngas concentration, heating value, and char yield are not affected by temperature linearly.

Temperature is the most significant factor for hydrogen production which is indicated by the high *F* value of 397.57. A high temperature enhances the extent of cracking of the WFG, which ultimately produces more hydrogen. The carrier gas flow

also affects the hydrogen production as a high concentration of hydrogen was obtained at a low carrier gas flow rate. The lack-of-fit value of 8.65 implies that it is not significant relative to the pure error. The adjusted (0.97) and predicted (0.94) *R*² values are in reasonable agreement which shows that the model fits well with the experimental data (please see the Table 3 footnote). This comparison is however done in the background when model reduction takes place. Adequate precision is a measure

of the signal-to-noise ratio. As per the requirement of the model, this ratio should be greater than 4 in order to show that the noise is not contributing any significant error in the response surface.¹⁹ In the present model, this value is 36.38 (see the Table 3 footnote), which is well above 4, thus indicating that the model does not have any significant error due to the noise.

Table 3 also describes the reduced quadratic models for the syngas concentration, char yield, and heating value of the product gas. All models are significant and have an insignificant lack-of-fit. As seen for hydrogen production, the same three parameters such as temperature, the second-order effect of temperature, and carrier gas flow rate also affect the syngas production. In the case of syngas production, also the adjusted (0.96) and predicted (0.91) R^2 values are in reasonable agreement which shows that the model fits well with the experimental data (see the Table 3 footnote). The adequate precision obtained by a model for syngas production is 29.3 (see the Table 3 footnote), which clearly indicates no significant error in the model due to noise.

In the case of char yield, the only significant factor is temperature. Both the effects of temperature (A) and the second-order effect of temperature (A^2) are significant. In case of char production, there might be a chance for error as the adequate precision value (10.2) is a little higher than that required by the model. Error in the char production was also indicated previously. To obtain the model for the heating value of the product gas, an inverse transformation of the response was performed and the two-level interaction of the temperature and carrier gas flow rate (AB) was retained (though not significant) in order to achieve an insignificant lack-of-fit. The model fits well in the case of the heating value as observed by the reasonable agreement of the adjusted and predicted R^2 values. The adequate precision value (29.8) is also quite high for the heating value (see the Table 3 footnote).

The following equations are the final empirical models in terms of actual factors for hydrogen, syngas, char, and product gas heating value.

$$\text{Hydrogen concentration (mol \%)} = 100.56 - 0.32A - 0.07B + (2.61 \times 10^{-4})A^2 \quad (3)$$

$$\text{Syngas concentration (mol \%)} = 86.40 - 0.25A - 0.08B + (2.17 \times 10^{-4})A^2 \quad (4)$$

$$\text{Char yield (g/100 g of WFG)} = 166.19 - 0.45A + (3.17 \times 10^{-4})A^2 \quad (5)$$

$$\begin{aligned} 1.0/(\text{heating value of product gas}) (\text{m}^3/\text{MJ}) = & 0.07 - (1.97 \times 10^{-4})A + (1.15 \times 10^{-4})Q + \\ & (1.67 \times 10^{-7})A^2 - (2.10 \times 10^{-7})AB \quad (6) \end{aligned}$$

where A = temperature in degrees Celcius, B = carrier gas flow rate in milliliters per minute, and A^2 = second-order effect of temperature.

To validate the models, the diagnostics section displays a normal plot of residuals (Figure 2) with the aim of elucidating whether all the errors are equally scattered. The residuals generally fall on a straight line which implies that the errors are distributed normally. The plots of residuals as a function of the predicted responses are given in Figure 3. There were no obvious patterns in all cases indicating that the models proposed are adequate and the ANOVA assumptions are met.

The three-dimensional (3-D) surface graphs for hydrogen, syngas, char production, and the heating value of the product

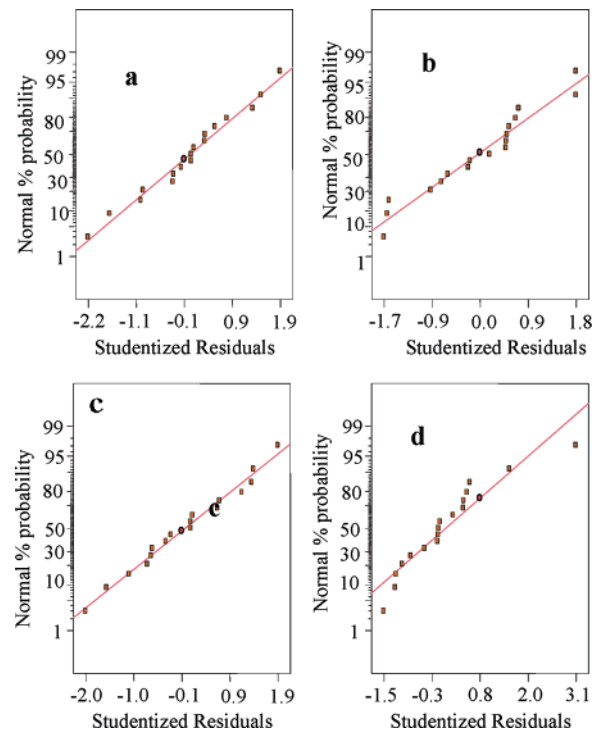


Figure 2. Normal probability plots for the residuals for (a) hydrogen concentration, (b) syngas concentration, (c) char yield, and (d) heating value of product gas.

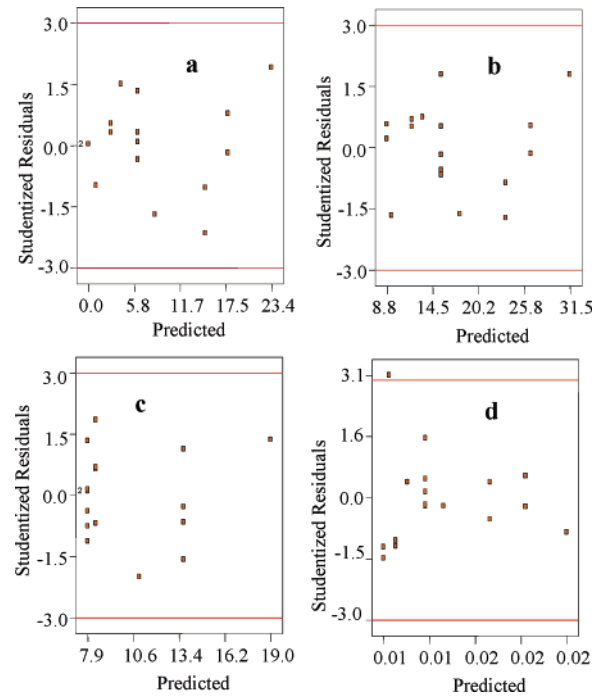


Figure 3. Plot of residual vs predicted response for (a) hydrogen concentration, (b) syngas concentration, (c) char yield, and (d) heating value of product gas.

gas are shown in Figures 4–7. These responses were depicted for different levels of temperature and carrier gas flow rate while keeping the packing particle size at the center level of 1.50 mm. All the plots have curvilinear profiles in accordance to the quadratic model fitted. It can be observed from Figure 4 that hydrogen production increased rapidly with an increase in temperature but slightly with a decrease in carrier gas flow rate. Temperature has a more pronounced effect on hydrogen production as described in the previous section. A similar trend

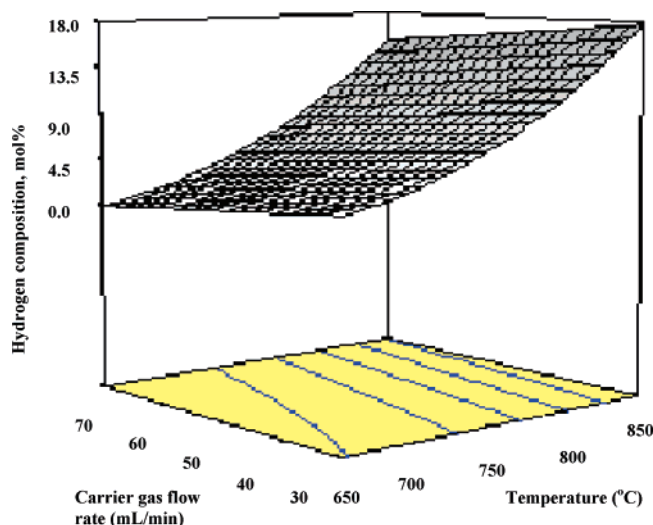


Figure 4. 3-D surface graphs for hydrogen concentration.

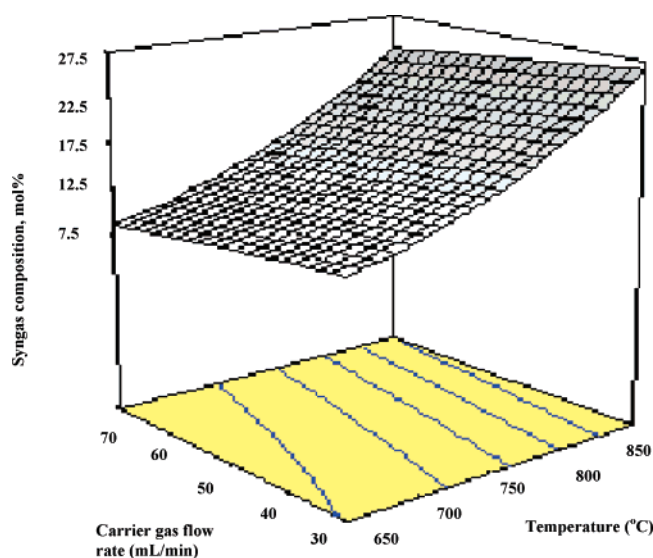


Figure 5. 3-D surface graphs for syngas concentration.

was also observed for syngas production (Figure 5). As can be seen from Figure 6, temperature is the only significant factor affecting char yield. It is clear from Figure 6 that the char yield decreased with temperature to a minimum at about 750 °C. The higher yield of char at 650 °C than at 750 °C is due to the fact that some residues of WFG which are not gasified completely at 650 °C (not char) are retained in the reactor. However, as the temperature increased beyond 750 °C, the char yield again increased. The reason for the increase in char yield above a 750 °C reaction temperature is discussed in the next section.

It can be observed from Figure 7 that, for a fixed carrier gas flow rate, the heating value of the product gas decreased with an increase in the pyrolysis temperature. This is due to the fact that at higher temperatures more syngas is produced at the expense of hydrocarbons. As the heating value of the hydrogen/syngas was lower than that of hydrocarbons, the overall heating value of the product gas was low. On the other hand, at a fixed temperature, the heating value of the gas increased with an increase in carrier gas flow rate due to the formation of more hydrocarbons. The carrier gas flow rate has less significant effect on heating value than temperature. This might be due to the fact that, within the range of gas flow rates considered in this study, the sequence of reactions are not changed significantly, thus making the gas composition somewhat stable. A maximum

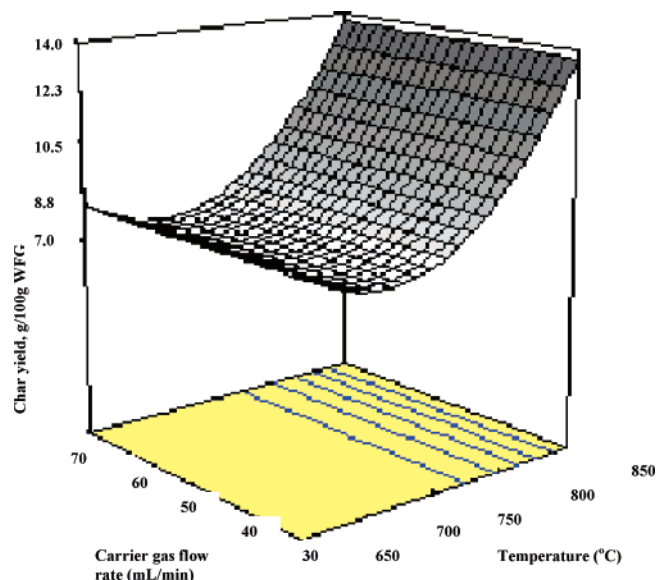


Figure 6. 3-D surface graphs for char yield.

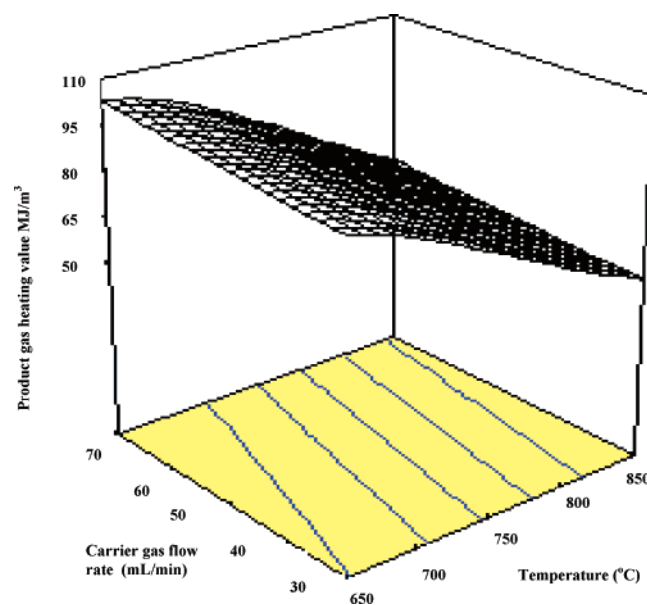


Figure 7. 3-D surface graphs for product gas heating value.

heating value of 104 MJ/m³ was observed at a temperature of 650 °C and a carrier gas flow rate of 70 mL/min.

4. Mechanism of Formation of Various Products during the Pyrolysis of WFG

Generally, triglycerides are the major component of any vegetable oil. During frying, oil undergoes many physical and chemical changes and therefore the part of the triglycerides gets oxidized and polymerized. Apart from this, many undesirable compounds are also formed after frying. Hence, the waste fryer grease is a complex mixture of triglycerides, diglycerides, monoglycerides, free fatty acids, oxidized and polymerized triglycerides, and many other compounds.²² Therefore, it is very difficult to derive the mechanism for the cracking of such a complex mixture. But, the mechanism of cracking of pure vegetable oil is well reported in the literature. Idem et al.¹³ have reported the mechanism for the cracking of canola oil in the

(22) Kulkarni, M. G.; Dalai, A. K. *Ind. Eng. Chem. Res.* **2006**, *45*, 2901–2913.

Table 4. Comparison of the Confirmation Experiment to Values Predicted by the Model

no.	packing particle size (mm)	temp (°C)	carrier gas flow rate (mL/min)	hydrogen conc (mol %)			syngas conc (mol %)			char yield (g/100 g WFG)		
				predicted	actual	error (%)	predicted	actual	error (%)	predicted	actual	error (%)
1	0.5	850	30	17.8	21.8	22.5	26.6	29.5	10.9	13.7	14.2	3.6
2	1.5	850	30	17.8	19.2	7.9	26.6	27.5	3.4	13.7	14.1	2.9
3	2.5	850	30	17.8	16.6	−6.7	26.6	25.1	−5.6	13.7	14.7	7.3

absence of catalyst. Since the canola oil is the major edible oil used in Canada, the waste fryer grease used in the present study contains canola oil as their major component with small amounts of animal fat and other vegetable oil. Even though the oil undergoes many changes during frying, triglycerides would remain as their major component.

On the basis of the reaction pathway derived for the cracking of triglyceride oil¹³ as well as for the present study, the major products formed after the thermal cracking of triglyceride oil are the following: gases (CO, CO₂, H₂, C_{1–4} hydrocarbon gases, dienes, C₅₊ hydrocarbon), organic liquid product (OLP) (aromatic hydrocarbon, heavy hydrocarbon), residual oil (after the vacuum distillation of OLP, the residual oil is left behind which contains high molecular weight components with boiling points higher than the temperature used for vacuum distillation), and coke.

The compositions of these products change depending on the operating conditions which were discussed in the earlier section.

Initially, canola oil decomposes at 240–300 °C to form saturated and unsaturated heavy oxygenated hydrocarbons which undergoes various reactions to form gas and liquid phase product. Saturated hydrocarbon decarbonylation and decarboxylation gives CO, CO₂, and hydrocarbon radicals. Unsaturated hydrocarbon undergoes C–C bond cleavage at the β position to C=C and gives C₄₊ dienes, hydrocarbon radicals, and short chain oxygenated hydrocarbon which on decarboxylation and decaronylation gives CO and CO₂ and further short chain hydrocarbon molecules. Hydrogen is one of the important gaseous products formed during the cracking of canola oil. Hydrogen is produced through various steps: (i) extraction of the proton during the formation of cycloolefins and aromatic hydrocarbon; (ii) coke formation by polymerization of olefins and aromatics; (iii) splitting of hydrocarbon molecules into their elements; (iv) dehydrogenation of olefins to diolefins and acetylenic hydrocarbon. On the other hand, hydrogen stabilizes the hydrocarbon radicals at various stages of the cracking process. Therefore, the hydrogen observed in the product is the difference between the amount produced and that which is consumed in stabilization of the hydrocarbon radicals. H₂ and CO produced by the above mechanisms are favored at the high temperature of 850 °C and carrier gas flow rate of 30 mL/min in the case of the present work. The detailed mechanism of pyrolysis of canola oil is described by Idem et al.¹³

Hydrocarbon radicals (saturated and unsaturated) that are formed during the formation of CO and CO₂ eliminate ethylene molecules followed by disproportionation, isomerization, and a subsequent hydrogen transfer reaction to give straight and branched chain C_{1–4} hydrocarbons. These compounds contribute to a high heating value of product gas. It was observed in the previous section that a maximum heating value of 104 MJ/m³ was observed at a temperature of 650 °C and a carrier gas flow rate of 70 mL/min. This may be due to the formation of large amounts of hydrocarbon by the mechanism as stated above. Char is one of the products formed during the thermal cracking of canola oil. The routes for the formation of char are due to the (i) decomposition of long chain hydrocarbon into its elements carbon and hydrogen, (ii) polymerization of olefins

and aromatic hydrocarbons, and (iii) polycondensation of canola oil and heavy oxygenated hydrocarbon molecules. Polyaromatic hydrocarbons are the intermediates in the formation of char from aromatic hydrocarbon. These materials are formed by successive elimination of hydrogen from aromatics and extensive removal of hydrogen from hydrocarbon resulting in char. In the present work, the reactions responsible for the formation of char are favored at temperatures above 750 °C.

4.2. Attaining Optimum Conditions for Hydrogen/Syngas Production. The numerical optimization of the pyrolysis process was done with a view towards maximizing the hydrogen and syngas concentrations in the product gas and minimizing char yield. Numerical optimization of these three responses within the specified range of process factors showed that a temperature of 850 °C and carrier gas flow rate of 30 mL/min is required to produce the maximum hydrogen concentration of 17.8 mol %, syngas concentration of 26.6 mol %, and minimum char yield of 13.7 g/100 g of WFG. The packing particle size had no effect on the optimization result.

The validity of the predicted model was examined by performing experiments at three different particle sizes at a temperature of 850 °C and carrier gas flow rate of 30 mL/min. The predicted and actual values for hydrogen and syngas concentration and the char yield are shown in Table 4. The percentage error range between the actual and the predicted value for hydrogen and syngas compositions and char yield are −6.7–22.5%, −5.6–10.9%, and 2.9–7.3%, respectively.

4.3. Steam Gasification of Waste Fryer Grease. The maximum hydrogen concentration obtainable by pyrolysis of WFG for the range of variables used was low. This is partly due to the low amount of hydrogen (11.2 wt %) in the WFG as obtained from the CHN analysis. The intent here is to improve on hydrogen production by cofeeding steam.

The optimum temperature of 850 °C, which is reported by the model for maximum hydrogen production by pyrolysis of WFG, was used for the steam gasification experiment. No carrier gas was used for the steam experiment since the most significant factor affecting hydrogen production was temperature and not the carrier gas flow rate. In addition, the steam provides an additional reduction in the residence time of the products in the reactor; a similar effect to that of the carrier gas.

The effects of the steam–carbon molar ratio (S/C) on hydrogen and syngas concentration in the product gas and the char yield at 850 °C are shown in Figure 8. The hydrogen production is seen to increase from 49.2 mol % at an S/C of 0.5 to a maximum of 56.2 mol % at an S/C of 1.5. A further increase in the S/C to 2.0 caused a decline in hydrogen production to 53.4 mol %. The syngas curve followed the same trend and was maximized (82.4 mol %) at an S/C of 1.5 and declined to 78.8 mol % at an S/C of 2.0. The high S/C ratio of 2.0 caused a further decrease in the residence time which is ultimately detrimental to both hydrogen and carbon monoxide production as the reactions responsible for their formation are further hindered in the reaction sequence.¹⁴

The char yield was observed to decrease from 38.9 to 12.1 g/100 g WFG as the S/C increased from 0.5 to 1.5 but increased slightly to 14.1 g/100 g WFG at an S/C of 2.0. By comparing

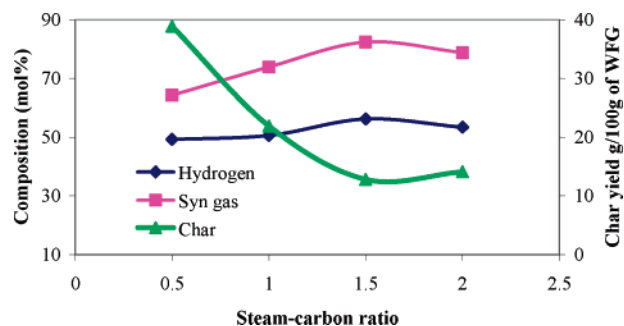


Figure 8. Effects of steam–carbon ratio on the concentration of hydrogen and syngas in the product gas during the steam gasification of waste fryer grease at 850 °C.

these results to those obtained during pyrolysis under the optimum conditions (Table 4), it can be inferred that the decline and subsequent increase in the char yield observed in Figure 8 is partly due to char gasification by steam and the decrease in residence time due to the increase in S/C. For example, the high char yield (38.9 g/100 g WFG) obtained at an S/C of 0.5 in Figure 8 was due to the high residence time of the volatiles in the reactor (which enhanced char formation) coupled with the fact that there was not sufficient steam to gasify the char. As the S/C increased, more steam was available for the steam carbon reaction, and therefore, the char yield decreased. Although more steam was available at an S/C of 2.0, there was a decrease in the residence time for the gasification of char, thus increasing the char yield.

5. Conclusion

The central composite circumscribed design proved to be effective for studying multivariable effects on pyrolysis. The pyrolysis of WFG was highly influenced by temperature. The carrier gas flow rate influenced both hydrogen and syngas production, but its effects were smaller than those of temperature. The quartz packing particle size had no significant effect on hydrogen, syngas, and char yield. The optimum condition for maximizing H₂ (17.8 mol %) and syngas (26.6 mol %) and minimizing char yield (13.7 g/100 g WFG) with pyrolysis of WFG was at 850 °C and with a carrier gas flow rate of 30 mL/min. The addition of steam drastically increased the hydrogen production to a maximum of 56.2 mol % and that of syngas to a maximum of 82.4 mol %. However, the char yield was reduced to 12.1 g/100 g of waste fryer grease.

Nomenclature

WFG: waste fryer grease
 GHG: green house gases
 FFA: free fatty acids
 CCR: conradson carbon residue
 WHSV: weight hourly space velocity
 RSM: response surface methodology
 CCC: central composite circumscribed
 ANOVA: analysis of variance

Acknowledgment. The authors are grateful to the Canada Research Chair (CRC) program for financial assistance to Dr. A.K. Dalai.

EF060238U